Acta Cryst. (1996). B52, 303–313

Four Polymorphs of a Cobaloxime Complex with Different Solid-State Photoisomerization Rates

KEIJU SAWADA,[a] DAISUKE HASHIZUME,[a] AKIKO SEKINE,[a] HIDEHIRO UEKUSA,[a] KOTARO KATO,[a] YUJI OHASHI,[a]* KAZUKO KAKINUMA[b] AND YOSHIAKI OHGO[b]

[a]*Department of Chemistry, Tokyo Institute of Technology O-okayama, Meguro-ku, Tokyo 152, Japan, and* [b]*Niigata College of Pharmacy, Kamishin-ei-cho, Niigata 950-21, Japan*

(*Received 15 May 1995; accepted 23 August 1995*)

Abstract

The complex (2-cyanoethyl)bis(dimethylglyoximato)-(triphenylphosphine)cobalt(III), $[Co(C_4H_7N_2O_2)_2(C_3H_4N)\{P(C_6H_5)_3\}]$, when it was crystallized rapidly from an aqueous methanol solution, has four crystal forms, three of which were obtained separately from different solvents in large amounts. The crystal structures of the four forms were determined by X-rays. The molecular structures in the four forms have different conformations around the Co—C and Co—P bonds. The packing energy calculation indicated that the four forms have approximately the same energy. The 2-cyanoethyl group of this complex was isomerized to the 1-cyanoethyl group when the powdered sample of the complex was irradiated with a xenon lamp. For three crystal forms prepared separately, the solid-state photoisomerization rates were measured from the change in the IR spectra, assuming first-order kinetics. A quantitative relationship between the rate constant and the size of the reaction cavity for the 2-cyanoethyl group has been obtained for the three crystal forms.

1. Introduction

The 2-cyanoethyl group bonded to the Co atom in the bis(dimethylglyoximato)cobalt(III), cobaloxime, complex has been found to be isomerized to the 1-cyanoethyl group upon exposure to visible light (Ohgo & Takeuchi, 1985). The photoisomerization proceeds only in the solid state and the reverse reaction has not been observed yet. Several cobaloxime complex crystals were prepared and the relation between the reaction rate and the crystal structure has been analyzed, changing the axial base ligand (Uchida, Danno, Sasada & Ohashi, 1987; Sekine, Ohashi & Hori, 1991; Sekine, Ohashi, Shimizu & Hori, 1991; Uchida, Ohashi & Ohgo, 1991). It has been found that three factors control the reaction rates: the hydrogen bond of the reactive group with the neighboring molecule, the conformation of the reactive group and the reaction cavity (Ohashi, Sekine, Shimizu, Hori & Uchida, 1990; Sekine & Ohashi, 1991). The reaction cavity, which is defined in the crystalline-state reaction (Ohashi, Yanagi, Kurihara, Sasada & Ohgo, 1981), represents the void space around the reactive group in the reactant crystal.

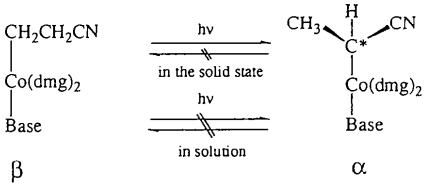

(I)

In these studies the powdered sample of the complex with triphenylphosphine as an axial base ligand gave a strange result; the sample obtained by rapid crystallization showed a significantly larger reaction rate than that of the sample obtained by slow crystallization, as shown in Fig. 1. Both samples, of course, contain no impurity. We analyzed all the crystals suitable for X-ray analysis in the rapid-crystallization sample. To our surprise, there are four crystal forms in the sample and only two forms were observed in the slow-crystallization sample. This brought about an idea that if four crystal forms would be obtained separately in large amounts, the reaction rate for each form may be measured and the relation between the rate and the crystal structure would be obtained. Herein we report the crystal structures of four forms and the relation between the reaction rate and structure.

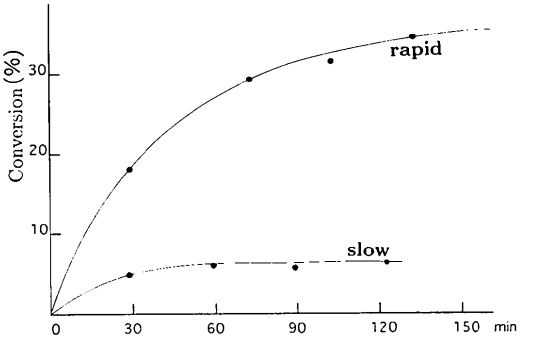

Fig. 1. Reaction rate of the two powdered samples obtained from rapid- and slow-crystallization samples.

2. Experimental

2.1. *Preparation of four crystal forms*

The complex was prepared in a similar way as reported previously (Schrauzer & Windgassen, 1967). The crude sample was saturated in an aqueous methanol solution at 353 K and was allowed to stand overnight at room temperature. Powdered crystals were obtained (rapid-crystallization sample). After several trials of recrystallization, well formed crystals were obtained (slow-crystallization sample). Since both the powdered samples of the rapid- and slow-crystallizations showed the same IR spectra, the preliminary experiments of photoisomerization, which were essentially the same as those described in the following section, were performed using both the powdered samples. The rates of isomerization are shown in Fig. 1. In order to explain the difference, crystals suitable for X-rays were picked up from the rapid-crystallization sample. 14 crystals were obtained. The preliminary X-ray works revealed that there are four crystal forms whose composition ratios are 1, 8, 1 and 4 for the (I), (II), (III) and (IV) forms, respectively. The crystal data of the four forms are given in Table 1. Ten crystals were selected from the slow-crystallization sample, having the same structure as that of form (II), except one crystal which was the same as form (I).

The crystallizations were then attempted to obtain each crystal form separately. The crystals of form (III) were obtained from a benzene solution. Form (II) was crystallized from an aqueous methanol solution with the addition of a small portion of sucrose. Sucrose was added to the solution in order to obtain form (IV), since it has the same space group as form (IV). However, it was found that the addition of sucrose is very effective to obtain pure form (II) crystals without the other forms. The reason has not yet been explained. Form (I) was obtained from an acetone solution. Although many trials were performed with a variety of solvents at different temperatures, form (IV) has not yet been obtained. Finally, an attempt to use the powder of crystal (IV), found in the rapid crystallization as seeds, was performed in vain. Although these four crystals have different space groups and unit-cell dimensions, the discrimination from their appearance on a microscope is very difficult, since the four crystal forms have similar color and shape.

2.2. *Crystal structure analysis*

The crystal data and experimental details are summarized in Table 1. The structures were solved by the direct method with the program *SHELXS*86 (Sheldrick, 1985) and refined by full-matrix least-squares using the program *SHELXL*93 (Sheldrick, 1993). The non-H atoms were refined with the anisotropic temperature factors. Some of the H atoms were located on the difference map and refined isotropically. The positions of the other H atoms were calculated and not refined. The 2-cyanoethyl groups in forms (III) and (IV) have disordered structures. They are refined with isotropic temperature factors under the constraint of having the same structure as observed in the related compounds. The occupancy factors of the disordered atoms were obtained in the refinement, assuming the corresponding atoms to have the same temperature factors. The weighting scheme was $w = [\sigma^2(F_o^2) + (aP)^2 + bP]^{-1}$, where $P = (F_o^2 + 2F_c^2)/3$ for all the crystals. The values of a and b for each crystal are given in Table 1. The atomic scattering factors including the dispersion terms were taken from *International Tables for Crystallography* (1992, Vol. C). Final atomic parameters are given in Tables 2, 3, 4 and 5 for (I), (II), (III) and (IV), respectively.*

2.3. *Photoisomerization*

For the measurement of the reaction rate, KBr disks which contained 1% of the 2-cyanoethyl complex were exposed to a 500 W xenon lamp (Ushio UXL-5S+UI-501C) through a 410 nm^{-1} band-pass filter, the distance between the disks and the lamp being 50 cm. The absorption assigned to the stretching vibrational mode of the cyano group of the 2-cyanoethyl complex, ν_{CN}, is at 2250 cm^{-1}, whereas ν_{CN} of the 1-cyanoethyl complex is at 2200 cm^{-1}. This indicates that the absorption band of ν_{CN} gradually changes from 2250 to 2200 cm^{-1}. The IR spectra of the KBr disks including the powdered samples of crystals (I), (II) and (III) were measured of intervals of 5 min, using a JASCO A-1000 IR spectrometer. The decrease of the absorption band at 2250 cm^{-1} within 50 min was well explained by first-order kinetics for each sample. The rate constant was obtained by least-squares fitting.

3. Results and discussion

3.1. *Crystal structure*

The crystal structures of (I), (II), (III) and (IV) are shown in Figs. 2, 3, 4 and 5, respectively. There are no unusually short contacts between the molecules. In order to compare the four crystal structures, the molecule is schematically drawn with a trigonal pyramid composed of the nitrogen of the 2-cyanoethyl group and the centers of three phenyl groups, and with a quadrilateral plate composed of four methyl groups of the equatorial ligands, as drawn in Fig. 6. The crystal structures of four forms are drawn schematically with the model in Fig. 7. The (I) and (II) forms are very similar to each other, although (II) has two crystallographically independent molecules, A and B, in an asymmetric unit. If A

* Lists of anisotropic displacement factors for non-H atoms, H-atom coordinates, complete geometry and structure factors have been deposited with the IUCr (reference: AS0694). Copies may be obtained through The Managing Editor, International Union of Crystallography, 5 Abbey Square, Chester CH1 2HU, England.

Table 1. *Experimental details*

	(I)	(II)	(III)	(IV)
Crystal data				
Chemical formula	$[Co(C_4H_7N_2O_2)_2(C_3H_4N)\{P(C_6H_5)_3\}]$	$[Co(C_4H_7N_2O_2)_2(C_3H_4N)\{P(C_6H_5)_3\}]$	$[Co(C_4H_7N_2O_2)_2(C_3H_4N)\{P(C_6H_5)_3\}]$	$[Co(C_4H_7N_2O_2)_2(C_3H_4N)\{P(C_6H_5)_3\}]$
Chemical formula weight	605.50	605.50	605.50	605.50
Cell setting	Monoclinic	Orthorhombic	Monoclinic	Orthorhombic
Space group	$P2_1/c$	*Pbca*	$P2_1/c$	$P2_12_12_1$
a (Å)	15.150 (5)	59.684 (8)	15.103 (8)	14.926 (4)
b (Å)	14.846 (6)	14.909 (2)	13.483 (9)	18.433 (4)
c (Å)	12.785 (3)	12.956 (2)	14.908 (5)	10.642 (5)
β (°)	93.26 (2)	90.0	107.12 (4)	90.0
V (Å^3)	2871 (2)	11 529 (3)	2901 (3)	2928 (2)
Z	4	16	4	4
D_x (Mg m^{-3})	1.401	1.395	1.386	1.374
Radiation type	Mo $K\alpha$	Cu $K\alpha$	Mo $K\alpha$	Mo $K\alpha$
Wavelength (Å)	0.71073	1.54184	0.71073	0.71073
No. of reflections for cell parameters	25	25	25	25
θ range (°)	10–15	22.5–30	20–22.5	10–15
μ (mm^{-1})	0.697	5.550	0.690	0.683
Temperature (K)	296	296	296	296
Crystal form	Prismatic	Prismatic	Prismatic	Prismatic
Crystal size (mm)	0.5 × 0.5 × 0.4	0.3 × 0.2 × 0.2	0.2 × 0.2 × 0.1	0.3 × 0.2 × 0.2
Crystal color	Dark orange	Dark orange	Dark orange	Dark orange
Data collection				
Diffractometer	AFC-7*S*	AFC-5*R*	AFC-7*S*	AFC-7*S*
Data collection method	$\omega/2\theta$	ω	$\omega/2\theta$	$\omega/2\theta$
Scan rate (° min^{-1})	4	8	4	4
Absorption correction	ψ scan	Integration	ψ scan	ψ scan
T_{min}	0.551	0.542	0.959	0.713
T_{max}	1.000	1.000	1.000	1.000
No. of measured reflections	7108	10 174	7183	3795
No. of independent reflections	6598	9194	6637	3769
No. of observed reflections	4557	4717	3415	1864
Criterion for observed reflections	$I > 2\sigma(I)$	$I > 2\sigma(I)$	$I > 2\sigma(I)$	$I > 2\sigma(I)$
θ_{max} (°)	27.5	62.5	27.5	27.5
Range of h, k, l	$0 \rightarrow h \rightarrow 19$ $0 \rightarrow k \rightarrow 19$ $-16 \rightarrow l \rightarrow 16$	$-5 \rightarrow h \rightarrow 68$ $-16 \rightarrow k \rightarrow 17$ $-14 \rightarrow l \rightarrow 10$	$0 \rightarrow h \rightarrow 19$ $0 \rightarrow k \rightarrow 17$ $-19 \rightarrow l \rightarrow 18$	$0 \rightarrow h \rightarrow 19$ $0 \rightarrow k \rightarrow 23$ $0 \rightarrow l \rightarrow 13$
No. of standard reflections	3	3	3	3
Frequency of standard reflections	Every 100 reflections	Every 100 reflections	Every 100 reflections	Every 100 reflections
Intensity decay (%)	−0.76	−1.01	−0.91	−2.78
Refinement				
Refinement on	F^2	F^2	F^2	F^2
$R[F^2 > 2\sigma(F^2)]$	0.0798	0.0597	0.0598	0.0663
$wR(F^2)$	0.2149	0.1276	0.1250	0.1437
S	1.187	1.138	1.169	0.981
No. of reflections used in refinement	5843	7500	5378	3097
No. of parameters used	374	738	365	386
H-atom treatment	Calculated	Calculated	Calculated	Calculated
Weighting scheme	$w = 1/[\sigma^2(F_o^2) + (0.1166P)^2 + 6.1755P]$, where $P = (F_o^2 + 2F_c^2)/3$	$w = 1/[\sigma^2(F_o^2) + (0.0680P)^2]$, where $P = (F_o^2 + 2F_c^2)/3$	$w = 1/[\sigma^2(F_o^2) + (0.0523P)^2]$, where $P = (F_o^2 + 2F_c^2)/3$	$w = 1/[\sigma^2(F_o^2) + (0.0724P)^2]$, where $P = (F_o^2 + 2F_c^2)/3$
Weighting parameter				
a	0.1166	0.0680	0.0523	0.0724
b	0.1755	0.0	0.0	0.0
$(\Delta/\sigma)_{max}$	−0.152	<0.001	−0.006	0.006
$\Delta\rho_{max}$ (e Å^{-3})	1.203	0.339	0.638	0.624
$\Delta\rho_{min}$ (e Å^{-3})	−0.838	−0.550	−0.496	−0.645
Extinction method	None	*SHELXL*93 (Sheldrick, 1993)	*SHELXL*93 (Sheldrick, 1993)	*SHELXL*93 (Sheldrick, 1993)
Extinction coefficient	–	0.213 × 10^{-3}	0.263 × 10^{-3}	0.241 × 10^{-3}
Source of atomic scattering factors	*International Tables for Crystallography* (1992, Vol. C)	*International Tables for Crystallography* (1992, Vol. C)	*International Tables for Crystallography* (1992, Vol. C)	*International Tables for Crystallography* (1992, Vol. C)

and *B* take the same conformation, the two forms cannot be distinguished. Forms (I) and (II) have larger density than (III) and (IV). Form (III) shows a head-to-tail packing, whereas forms (I) and (II) are head-to-head. The packing mode of (IV) is quite different from the others, although the head-to-tail pairs are made separately.

Table 2. *Fractional atomic coordinates and equivalent isotropic displacement parameters (Å²) for (I)*

$U_{eq} = (1/3)\Sigma_i\Sigma_j U_{ij} a_i^* a_j^* \mathbf{a}_i.\mathbf{a}_j.$

	x	y	z	U_{eq}
Co(1)	0.7441 (1)	0.3597 (1)	0.8315 (1)	0.032
P(1)	0.7537 (1)	0.5174 (1)	0.7963 (1)	0.032
O(1)	0.7011 (3)	0.3733 (3)	1.0435 (3)	0.055
O(2)	0.6263 (3)	0.3355 (3)	0.6520 (3)	0.051
O(3)	0.7856 (3)	0.3311 (3)	0.6201 (3)	0.054
O(4)	0.8619 (3)	0.3701 (3)	1.0130 (3)	0.058
N(1)	0.6693 (3)	0.3721 (3)	0.9427 (3)	0.039
N(2)	0.6336 (3)	0.3515 (3)	0.7560 (3)	0.039
N(3)	0.8169 (3)	0.3391 (3)	0.7211 (3)	0.039
N(4)	0.8540 (3)	0.3595 (3)	0.9077 (3)	0.043
N(5)	0.7332 (5)	−0.0043 (4)	0.8337 (6)	0.095
C(1)	0.5855 (4)	0.3735 (4)	0.9211 (5)	0.047
C(2)	0.5644 (4)	0.3641 (4)	0.8089 (5)	0.045
C(3)	0.9012 (4)	0.3339 (4)	0.7428 (5)	0.046
C(4)	0.9235 (4)	0.3456 (4)	0.8553 (5)	0.047
C(5)	0.5200 (5)	0.3738 (6)	1.0048 (7)	0.076
C(6)	0.4726 (4)	0.3693 (6)	0.7576 (7)	0.081
C(7)	0.9670 (5)	0.3188 (5)	0.6631 (6)	0.070
C(8)	1.0153 (4)	0.3393 (6)	0.9047 (7)	0.077
C(9)	0.7366 (4)	0.2259 (3)	0.8646 (4)	0.044
C(10)	0.7425 (5)	0.1637 (4)	0.7744 (5)	0.057
C(11)	0.7349 (5)	0.0684 (4)	0.8069 (6)	0.065
C(12)	0.6618 (3)	0.5573 (3)	0.7082 (4)	0.036
C(13)	0.5947 (4)	0.6057 (4)	0.7494 (5)	0.054
C(14)	0.5230 (5)	0.6361 (5)	0.6853 (7)	0.071
C(15)	0.5188 (5)	0.6155 (5)	0.5802 (7)	0.073
C(16)	0.5852 (5)	0.5658 (5)	0.5405 (5)	0.067
C(17)	0.6536 (4)	0.5334 (4)	0.6035 (5)	0.051
C(18)	0.7548 (3)	0.6025 (3)	0.9017 (4)	0.039
C(19)	0.7638 (5)	0.6919 (4)	0.8752 (4)	0.058
C(20)	0.7600 (5)	0.7585 (4)	0.9501 (5)	0.067
C(21)	0.7484 (5)	0.7358 (5)	1.0531 (5)	0.062
C(22)	0.7414 (4)	0.6470 (4)	1.0793 (4)	0.051
C(23)	0.7449 (4)	0.5800 (4)	1.0041 (4)	0.042
C(24)	0.8568 (3)	0.5460 (3)	0.7364 (4)	0.038
C(25)	0.8669 (4)	0.5578 (4)	0.6299 (4)	0.052
C(26)	0.9488 (5)	0.5756 (5)	0.5919 (6)	0.068
C(27)	1.0218 (5)	0.5813 (5)	0.6571 (6)	0.069
C(28)	1.0145 (4)	0.5691 (5)	0.7643 (6)	0.067
C(29)	0.9333 (4)	0.5529 (5)	0.8022 (5)	0.056

3.2. *Molecular structure*

The molecular structures of (I), (II), (III) and (IV), with atom numbering, are shown in Figs. 8, 9, 10 and 11, respectively. Selected bond distances and angles are listed in Table 6. Bond distances and angles are in good agreement with the corresponding values in the related complexes. The 2-cyanoethyl groups in (III) and (IV) are disordered; the ratios of major and minor parts are 0.75:0.25 for (III) and 0.59:0.41 for (IV), respectively. The 2-cyanoethyl groups in all the crystals take perpendicular conformations to the cobaloxime plane. The torsion angles of Co—C(9)—C(10)—C(11) are −179.1 (5), 177.7 (5), −179.9 (4), −171.5 (5), 171.5 (11), 180.0 (10) and 163.7 (14)° for (I), (II*A*), (II*B*), (III), (III′), (IV) and (IV′), respectively, where (III′) and (IV′) denote the minor parts of the disordered molecules. For the complex with pyridine as an axial base ligand, two crystal forms were obtained (Zangrando, Bresciani-Pahor, Randaccio, Charland & Marzilli, 1986; Uchida, Ohashi & Ohgo, 1991). Although the 2-cyanoethyl group in one form takes a perpendicular

Table 3. *Fractional atomic coordinates and equivalent isotropic displacement parameters (Å²) for (II)*

$U_{eq} = (1/3)\Sigma_i\Sigma_j U_{ij} a_i^* a_j^* \mathbf{a}_i.\mathbf{a}_j.$

	x	y	z	U_{eq}
Co(1*A*)	0.3127 (1)	0.6417 (1)	0.7480 (1)	0.032
P(1*A*)	0.3093 (1)	0.4820 (1)	0.7494 (1)	0.028
O(1*A*)	0.3193 (1)	0.6589 (3)	0.5317 (3)	0.047
O(2*A*)	0.3458 (1)	0.6333 (3)	0.9047 (3)	0.056
O(3*A*)	0.3063 (1)	0.6303 (3)	0.9638 (3)	0.050
O(4*A*)	0.2802 (1)	0.6696 (3)	0.5919 (3)	0.056
N(1*A*)	0.3288 (1)	0.6458 (3)	0.6244 (3)	0.040
N(2*A*)	0.3418 (1)	0.6345 (3)	0.8018 (4)	0.040
N(3*A*)	0.2962 (1)	0.6428 (3)	0.8720 (3)	0.038
N(4*A*)	0.2838 (1)	0.6600 (3)	0.6943 (4)	0.038
N(5*A*)	0.3178 (1)	1.0030 (4)	0.7104 (5)	0.081
C(1*A*)	0.3507 (1)	0.6386 (4)	0.6299 (5)	0.050
C(2*A*)	0.3581 (1)	0.6314 (4)	0.7368 (5)	0.045
C(3*A*)	0.2744 (1)	0.6557 (4)	0.8654 (5)	0.043
C(4*A*)	0.2676 (1)	0.6680 (4)	0.7592 (5)	0.042
C(5*A*)	0.3658 (1)	0.6439 (5)	0.5384 (5)	0.075
C(6*A*)	0.3822 (1)	0.6232 (5)	0.7699 (6)	0.083
C(7*A*)	0.2595 (1)	0.6559 (4)	0.9566 (5)	0.065
C(8*A*)	0.2438 (1)	0.6882 (4)	0.7303 (5)	0.068
C(9*A*)	0.3154 (1)	0.7782 (4)	0.7707 (5)	0.059
C(10*A*)	0.3161 (1)	0.8303 (5)	0.6808 (6)	0.085
C(11*A*)	0.3172 (1)	0.9302 (5)	0.6992 (5)	0.062
C(12*A*)	0.3314 (1)	0.4327 (4)	0.8292 (4)	0.035
C(13*A*)	0.3499 (1)	0.3932 (4)	0.7813 (5)	0.048
C(14*A*)	0.3677 (1)	0.3635 (4)	0.8391 (6)	0.062
C(15*A*)	0.3675 (1)	0.3713 (4)	0.9448 (6)	0.061
C(16*A*)	0.3497 (1)	0.4090 (4)	0.9937 (5)	0.055
C(17*A*)	0.3317 (1)	0.4422 (4)	0.9369 (4)	0.043
C(18*A*)	0.3104 (1)	0.4112 (4)	0.6346 (4)	0.036
C(19*A*)	0.3083 (1)	0.3187 (4)	0.6468 (5)	0.052
C(20*A*)	0.3085 (1)	0.2626 (4)	0.5628 (5)	0.064
C(21*A*)	0.3102 (1)	0.2965 (5)	0.4650 (5)	0.069
C(22*A*)	0.3117 (1)	0.3871 (5)	0.4507 (5)	0.061
C(23*A*)	0.3119 (1)	0.4442 (4)	0.5355 (4)	0.045
C(24*A*)	0.2818 (1)	0.4491 (3)	0.7980 (4)	0.031
C(25*A*)	0.2769 (1)	0.4231 (4)	0.8974 (5)	0.048
C(26*A*)	0.2547 (1)	0.4084 (4)	0.9271 (5)	0.064
C(27*A*)	0.2377 (1)	0.4192 (5)	0.8596 (6)	0.071
C(28*A*)	0.2422 (1)	0.4436 (5)	0.7594 (6)	0.067
C(29*A*)	0.2642 (1)	0.4587 (4)	0.7293 (5)	0.049
Co(1*B*)	0.0639 (1)	0.6420 (1)	0.8490 (1)	0.027
P(1*B*)	0.0615 (1)	0.4847 (1)	0.8121 (1)	0.028
O(1*B*)	0.0749 (1)	0.6239 (3)	1.0609 (3)	0.048
O(2*B*)	0.0937 (1)	0.6692 (3)	0.6811 (3)	0.046
O(3*B*)	0.0532 (1)	0.6733 (3)	0.6390 (3)	0.047
O(4*B*)	0.0341 (1)	0.6288 (3)	1.0202 (3)	0.054
N(1*B*)	0.0827 (1)	0.6262 (3)	0.9645 (3)	0.035
N(2*B*)	0.0917 (1)	0.6509 (3)	0.7820 (3)	0.036
N(3*B*)	0.0453 (1)	0.6638 (3)	0.7349 (3)	0.033
N(4*B*)	0.0361 (1)	0.6412 (3)	0.9165 (3)	0.037
N(5*B*)	0.0677 (1)	1.0042 (4)	0.8505 (6)	0.098
C(1*B*)	0.1043 (1)	0.6239 (4)	0.9452 (5)	0.042
C(2*B*)	0.1096 (1)	0.6364 (4)	0.8370 (4)	0.039
C(3*B*)	0.0238 (1)	0.6687 (4)	0.7531 (5)	0.043
C(4*B*)	0.0184 (1)	0.6556 (4)	0.8619 (5)	0.042
C(8*B*)	−0.0048 (1)	0.6609 (5)	0.9031 (6)	0.079
C(7*B*)	0.0070 (1)	0.6834 (4)	0.6689 (5)	0.072
C(6*B*)	0.1325 (1)	0.6315 (4)	0.7925 (6)	0.072
C(5*B*)	0.1210 (1)	0.6185 (4)	1.0311 (5)	0.072
C(9*B*)	0.0663 (1)	0.7755 (3)	0.8819 (4)	0.041
C(10*B*)	0.0650 (1)	0.8381 (4)	0.7918 (5)	0.052
C(11*B*)	0.0669 (1)	0.9324 (5)	0.8232 (5)	0.058
C(12*B*)	0.0850 (1)	0.4478 (3)	0.7321 (4)	0.034
C(13*B*)	0.1020 (1)	0.3961 (4)	0.7735 (5)	0.053
C(14*B*)	0.1199 (1)	0.3704 (5)	0.7158 (6)	0.075
C(15*B*)	0.1216 (1)	0.3953 (5)	0.6143 (6)	0.074
C(16*B*)	0.1052 (1)	0.4464 (4)	0.5715 (5)	0.060
C(17*B*)	0.0871 (1)	0.4760 (4)	0.6300 (4)	0.043
C(18*B*)	0.0614 (1)	0.3975 (3)	0.9133 (4)	0.034
C(19*B*)	0.0589 (1)	0.3085 (4)	0.8854 (5)	0.052
C(20*B*)	0.0605 (1)	0.2424 (4)	0.9582 (5)	0.064

Table 3 (*cont.*)

	x	*y*	*z*	U_{eq}
C(21*B*)	0.0643 (1)	0.2637 (4)	1.0598 (5)	0.061
C(22*B*)	0.0660 (1)	0.3500 (4)	1.0901 (4)	0.046
C(23*B*)	0.0649 (1)	0.4184 (4)	1.0165 (4)	0.039
C(24*B*)	0.0355 (1)	0.4559 (3)	0.7446 (4)	0.032
C(25*B*)	0.0336 (1)	0.4430 (4)	0.6391 (4)	0.049
C(26*B*)	0.0126 (1)	0.4260 (5)	0.5955 (5)	0.063
C(27*B*)	−0.0060 (1)	0.4201 (5)	0.6545 (6)	0.068
C(28*B*)	−0.0043 (1)	0.4324 (4)	0.7582 (6)	0.063
C(29*B*)	0.0162 (1)	0.4497 (4)	0.8037 (4)	0.045

conformation to the cobaloxime plane, as observed in the triphenylphosphine complex, it has a parallel conformation to the cobaloxime plane in another form. The torsion angles of Co—C(9)—C(10)—C(11) are −173.2 (5) and 85.8 (7)° for perpendicular and parallel conformations, respectively.

The torsion angles around the Co—C bond of the 2-cyanoethyl groups are scattered in a wide range. The torsion angles of N(1)—Co—C(9)—C(10) are 148.5 (5), 31.8 (6), 149.0 (5), 4.1 (5), −46.5 (11), 6.7 (11) and −77.3 (13)° for (I), (II*A*), (II*B*), (III), (III′), (IV) and (IV′), respectively. On the other hand, the triphenylphospine moieties in the four forms take similar conformations; one phenyl ring, C(18)–C(23), is almost perpendicular to the cobaloxime plane and the other two rings are almost parallel to the plane. Moreover, the torsion angles around the Co—P bond are in a fairly narrow range; the N(2)—Co—P—C(12) angles are −4.8 (8), 15.0 (2), −4.2 (2), −29.2 (2) and −7.4 (4)° for (I), (II*A*), (II*B*), (III) and (IV), respectively.

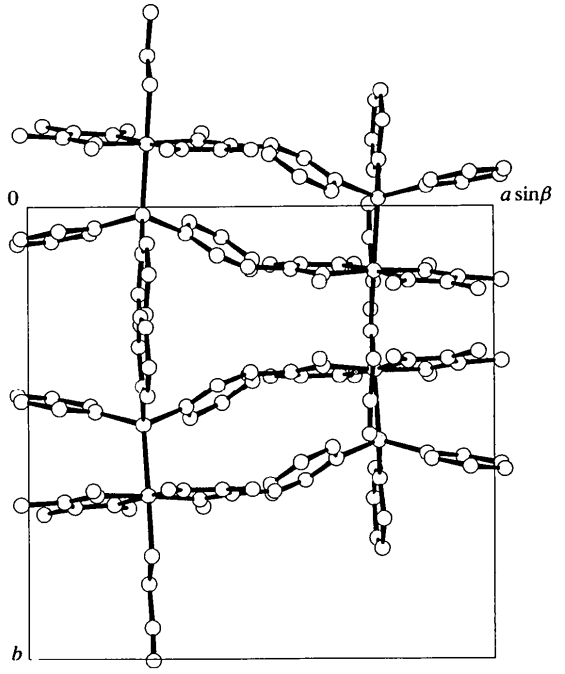

Fig. 2. Crystal structure of (I) viewed down the *c* axis.

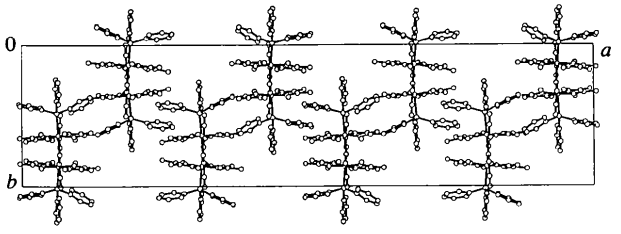

Fig. 3. Crystal structure of (II) viewed down the *c* axis.

Table 4. *Fractional atomic coordinates and equivalent isotropic displacement parameters (Å²) for (III)*

$U_{eq} = (1/3)\Sigma_i\Sigma_j U_{ij} a_i^* a_j^* \mathbf{a}_i.\mathbf{a}_j.$

	x	*y*	*z*	U_{eq}/U_{iso}
Co(1)	0.7469 (1)	0.9264 (1)	0.8263 (1)	0.028
P(1)	0.7497 (1)	0.9062 (1)	0.6678 (1)	0.027
O(1)	0.7857 (2)	1.1322 (2)	0.8393 (2)	0.042
O(2)	0.5725 (2)	0.8307 (3)	0.7834 (3)	0.061
O(3)	0.7101 (3)	0.7203 (3)	0.8394 (3)	0.058
O(4)	0.9240 (2)	1.0214 (3)	0.8740 (2)	0.047
N(1)	0.7198 (2)	1.0624 (3)	0.8144 (2)	0.032
N(2)	0.6172 (3)	0.9177 (3)	0.7889 (3)	0.040
N(3)	0.7753 (3)	0.7897 (3)	0.8484 (3)	0.039
N(4)	0.8767 (2)	0.9350 (3)	0.8672 (2)	0.033
N(5*A*)*	0.7411 (5)	1.0218 (6)	1.1794 (4)	0.048 (2)
N(5*B*)*	0.7719 (18)	1.003 (2)	1.1901 (12)	0.044 (2)
C(1)	0.6325 (3)	1.0864 (4)	0.7823 (3)	0.041
C(2)	0.5718 (3)	1.0006 (4)	0.7666 (4)	0.048
C(3)	0.8630 (4)	0.7670 (4)	0.8776 (3)	0.044
C(4)	0.9219 (3)	0.8536 (4)	0.8878 (3)	0.041
C(5)	0.5994 (4)	1.1912 (4)	0.7672 (4)	0.065
C(6)	0.4684 (3)	1.0044 (5)	0.7304 (5)	0.081
C(7)	0.8960 (5)	0.6615 (4)	0.8973 (4)	0.074
C(8)	1.0252 (4)	0.8465 (5)	0.9193 (4)	0.064
C(9)	0.7449 (4)	0.9288 (3)	0.9611 (3)	0.047
C(10*A*)*	0.7182 (5)	1.0254 (4)	0.9998 (3)	0.051 (2)
C(10*B*)*	0.7966 (15)	1.0117 (12)	1.0251 (10)	0.052 (2)
C(11*A*)*	0.7323 (5)	1.0227 (6)	1.1016 (4)	0.051 (2)
C(11*B*)*	0.7756 (16)	1.0097 (19)	1.1156 (12)	0.050 (2)
C(12)	0.6509 (3)	0.8322 (3)	0.6019 (3)	0.030
C(13)	0.5742 (3)	0.8807 (4)	0.5437 (4)	0.049
C(14)	0.4943 (4)	0.8299 (4)	0.4977 (4)	0.061
C(15)	0.4886 (4)	0.7305 (4)	0.5092 (4)	0.060
C(16)	0.5621 (4)	0.6806 (4)	0.5679 (4)	0.053
C(17)	0.6419 (3)	0.7313 (3)	0.6157 (3)	0.041
C(18)	0.7476 (3)	1.0118 (3)	0.5886 (3)	0.031
C(19)	0.7409 (3)	0.9919 (4)	0.4948 (3)	0.044
C(20)	0.7495 (4)	1.0671 (4)	0.4353 (4)	0.054
C(21)	0.7652 (3)	1.1634 (4)	0.4684 (4)	0.058
C(22)	0.7717 (3)	1.1840 (4)	0.5607 (4)	0.051
C(23)	0.7635 (3)	1.1083 (3)	0.6212 (4)	0.041
C(24)	0.8585 (3)	0.8479 (3)	0.6624 (3)	0.033
C(25)	0.8723 (4)	0.7481 (4)	0.6581 (4)	0.054
C(26)	0.9600 (4)	0.7114 (4)	0.6607 (4)	0.069
C(27)	1.0326 (4)	0.7745 (5)	0.6685 (4)	0.065
C(28)	1.0194 (4)	0.8741 (5)	0.6732 (4)	0.058
C(29)	0.9332 (3)	0.9103 (4)	0.6701 (4)	0.045

* The occupancy factors of groups *A* and *B* are 0.75 and 0.25, respectively.

3.3. *Potential energy calculation*

In order to examine the conformational variation in the four crystal forms, the potential energy for each isolated molecule was calculated with the program *WMIN* (Busing, 1981), rotating the 2-cyanoethyl group around the Co—C(9) bond, the cyano group around the C(9)—C(10) bond and the triphenylphosphine moiety

around the Co—P bond. The rotation around a bond was performed with the other two rotations fixed. The potential energy is obtained by summing up the interactions of the nonbonded atom pairs expressed as exp-6 functions (Williams & Starr, 1977). Before the calculation the positions of the H atoms were corrected

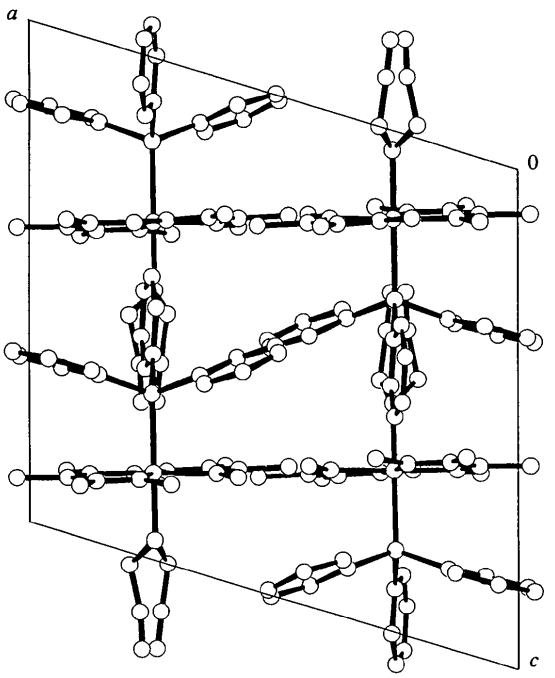

Fig. 4. Crystal structure of (III) viewed down the *b* axis.

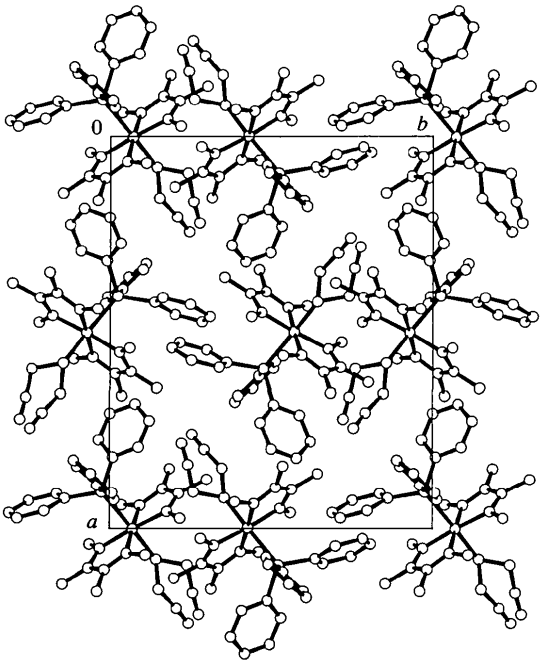

Fig. 5. Crystal structure of (IV) viewed along the *c* axis.

Table 5. *Fractional atomic coordinates and equivalent isotropic displacement parameters (Å²) for (IV)*

$U_{eq} = (1/3)\Sigma_i\Sigma_j U_{ij} a_i^* a_j^* \mathbf{a}_i.\mathbf{a}_j.$

	x	*y*	*z*	U_{eq}/U_{iso}
Co(1)	0.0713 (1)	0.0012 (1)	0.5392 (1)	0.038
P(1)	−0.0240 (2)	−0.0932 (1)	0.4582 (2)	0.035
O(1)	0.1108 (6)	0.0683 (4)	0.3069 (7)	0.064
O(2)	−0.0611 (5)	0.0405 (4)	0.7168 (6)	0.060
O(3)	0.0381 (5)	−0.0604 (4)	0.7796 (6)	0.057
O(4)	0.2180 (5)	−0.0258 (4)	0.3756 (7)	0.065
N(1)	0.0533 (6)	0.0635 (4)	0.4035 (7)	0.047
N(2)	−0.0292 (6)	0.0517 (4)	0.6013 (8)	0.050
N(3)	0.0937 (6)	−0.0592 (4)	0.6793 (7)	0.044
N(4)	0.1771 (6)	−0.0436 (5)	0.4844 (8)	0.051
N(5*A*)*	0.2464 (15)	0.2411 (12)	0.715 (2)	0.102 (8)
N(5*B*)*	0.2770 (19)	0.2181 (12)	0.682 (3)	0.110 (10)
C(1)	−0.0154 (8)	0.1051 (5)	0.4071 (11)	0.055
C(2)	−0.0646 (7)	0.1005 (5)	0.5266 (11)	0.052
C(3)	0.1636 (7)	−0.1017 (5)	0.6731 (9)	0.046
C(4)	0.2141 (7)	−0.0896 (6)	0.5618 (11)	0.055
C(5)	−0.0378 (8)	0.1610 (6)	0.3091 (13)	0.079
C(6)	−0.1450 (7)	0.1420 (7)	0.5598 (14)	0.082
C(7)	0.1857 (7)	−0.1545 (6)	0.7727 (11)	0.067
C(8)	0.2995 (7)	−0.1271 (7)	0.5314 (14)	0.083
C(9)	0.1445 (8)	0.0791 (5)	0.6271 (11)	0.073
C(10*A*)*	0.1524 (12)	0.1556 (7)	0.5725 (17)	0.071 (5)
C(10*B*)*	0.2417 (9)	0.0915 (12)	0.587 (2)	0.071 (5)
C(11*A*)*	0.2080 (13)	0.2040 (14)	0.6499 (19)	0.090 (9)
C(11*B*)*	0.2584 (15)	0.1633 (13)	0.642 (3)	0.092 (11)
C(12)	−0.1382 (6)	−0.0774 (5)	0.5114 (8)	0.036
C(13)	−0.2008 (7)	−0.0458 (5)	0.4330 (10)	0.050
C(14)	−0.2842 (7)	−0.0268 (6)	0.4759 (12)	0.057
C(15)	−0.3086 (7)	−0.0406 (6)	0.5991 (13)	0.062
C(16)	−0.2484 (7)	−0.0719 (5)	0.6792 (11)	0.052
C(17)	−0.1620 (7)	−0.0893 (5)	0.6397 (9)	0.046
C(18)	−0.0380 (7)	−0.1112 (5)	0.2894 (8)	0.042
C(19)	−0.1012 (8)	−0.1607 (6)	0.2492 (10)	0.063
C(20)	−0.1103 (9)	−0.1759 (7)	0.1211 (12)	0.076
C(21)	−0.0572 (10)	−0.1416 (8)	0.0365 (12)	0.083
C(22)	0.0071 (11)	−0.0911 (9)	0.0737 (10)	0.087
C(23)	0.0134 (8)	−0.0735 (7)	0.2021 (10)	0.062
C(24)	0.0099 (6)	−0.1840 (4)	0.5075 (8)	0.036
C(25)	−0.0330 (8)	−0.2280 (5)	0.5936 (10)	0.056
C(26)	0.0020 (8)	−0.2953 (5)	0.6272 (11)	0.065
C(27)	0.0800 (9)	−0.3183 (6)	0.5767 (11)	0.065
C(28)	0.1230 (8)	−0.2763 (5)	0.4878 (10)	0.058
C(29)	0.0892 (7)	−0.2092 (5)	0.4560 (10)	0.052

* The occupancy factors of groups *A* and *B* are 0.59 and 0.41, respectively.

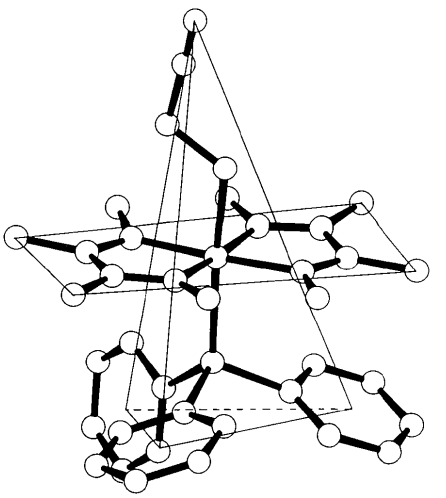

Fig. 6. Molecular model expressed by a pyramid and a plate.

Table 6. *Selected bond distances and angles of the molecules in four crystal forms*

(IIA) and (II*B*) are *A* and *B* molecules in (II), and (III′) and (IV′) are the minor part molecules of the disordered ones in (III) and (IV), respectively.

	(I)	(IIA)	(II*B*)	(III)	(III′)	(IV)	(IV′)
Co(1)—P(1)	2.391 (2)	2.390 (2)	2.397 (2)	2.391 (2)		2.408 (3)	
Co(1)—C(9)	2.036 (5)	2.063 (6)	2.041 (5)	2.020 (5)		2.026 (10)	
C(9)—C(10)	1.484 (8)	1.401 (8)	1.496 (7)	1.525 (3)	1.527 (3)	1.5298 (11)	1.5298 (11)
C(10)—C(11)	1.481 (9)	1.509 (9)	1.468 (8)	1.470 (3)	1.473 (3)	1.4709 (10)	1.4708 (11)
N(1)—Co(1)—P(1)	95.28 (13)	94.7 (2)	94.13 (14)	94.89 (11)		94.8 (2)	
N(2)—Co(1)—P(1)	91.67 (13)	91.0 (2)	91.67 (14)	91.11 (13)		90.5 (2)	
N(3)—Co(1)—P(1)	88.46 (13)	87.65 (14)	88.66 (13)	89.52 (11)		87.8 (2)	
N(4)—Co(1)—P(1)	92.14 (14)	94.10 (14)	91.99 (14)	90.43 (12)		94.0 (3)	
N(1)—Co(1)—C(9)	84.0 (2)	92.8 (2)	85.1 (2)	90.7 (2)		89.8 (4)	
N(2)—Co(1)—C(9)	89.1 (2)	86.0 (2)	88.0 (2)	88.6 (2)		85.5 (4)	
N(3)—Co(1)—C(9)	92.3 (2)	84.8 (2)	92.1 (2)	84.9(2)		87.6 (4)	
N(4)—Co(1)—C(9)	87.1 (2)	89.0 (2)	88.4 (2)	89.8 (2)		90.0 (4)	
C(11)—C(10)—C(9)	111.6 (5)	114.7 (6)	112.2 (5)	113.3 (5)	110.5 (14)	112.8 (13)	101.3 (12)
C(10)—C(9)—Co(1)	116.0 (4)	115.5 (5)	116.3 (4)	118.2 (3)	118.6 (7)	121.6 (8)	119.7 (10)
C(9)—Co(1)—P(1)	178.8 (2)	171.3 (2)	179.2 (2)	174.34 (13)		173.4 (3)	
Co(1)—P(1)—C(12)	112.2 (2)	110.2 (2)	111.3 (2)	110.23 (14)		109.0 (3)	

for the ideal geometries. Fig. 12 shows the potential energy curve with the torsion angle around the Co—C(9) bond. There are two low-energy regions; one is a narrow region around −150°, the other is a fairly wide region from 0 to 100°. All the conformations, including the disordered of the four crystal forms, are plotted in these two energy minimums and the energy difference among them is within 8.4 kJ mol^{-1}. Fig. 13 shows the potential

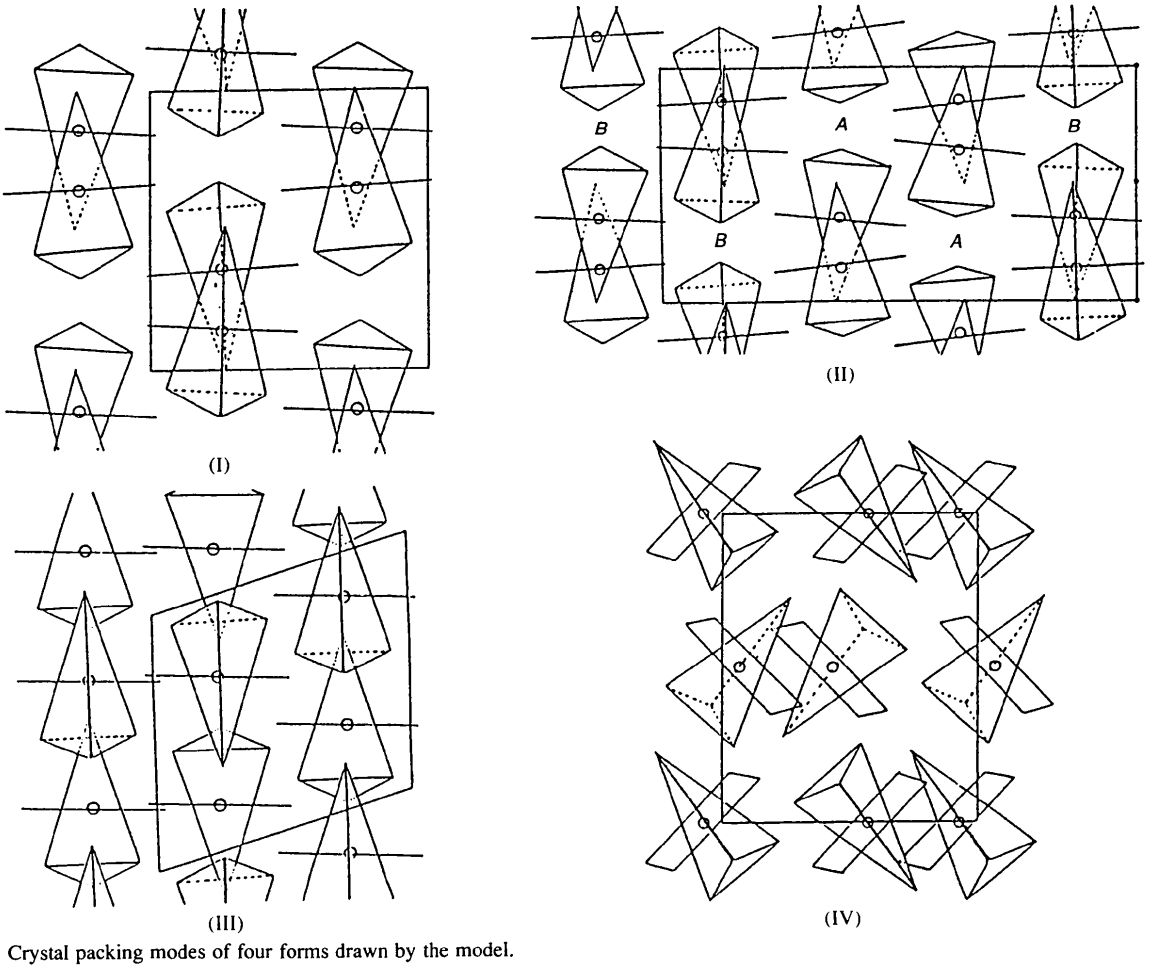

Fig. 7. Crystal packing modes of four forms drawn by the model.

energy curve for the torsional angle around the Co—P bond. There is only one potential minimum and all the conformations are included in the narrow region, the energy difference also being *ca* 8.4 kJ mol^{-1}. Fig. 14 shows the potential energy curve for the torsion angle around the C(9)—C(10) bond. There are three minimums, depending on the three substituents at C(9). All the torsion angles of the four crystal forms are in a narrow region around the perpendicular conformation. The torsion angle of one form of the pyridine complex occupies one of two parallel conformations. In this case the energy difference is within 8.4 kJ mol^{-1}. These results suggest that although the conformations around the single bonds are different in the four crystal forms due to the different crystal packing, the conformations with potential energy within 8.4 kJ mol^{-1} higher than its minimum value are permitted in the crystal structures.

The packing potential energies for four crystal forms were calculated with the program *WMIN* (Busing, 1981) using the same potential functions. It seems difficult to compare the energy of form (II) with those of the other crystal forms, since the form (II) crystal has two crystallographically independent molecules in an asymmetric unit. The packing energy was optimized by changing nine or ten parameters, that is, three translation and three libration parameters of the molecule and cell dimensions, *a*, *b* and *c* (and β for monoclinic system). The molecular structure was fixed to that in the crystal structure. For such rigid models, the packing energies were converged to −200.5, −190.0 and −188.0 kJ mol^{-1} for (I), (II) and (IV), respectively. The converged values of the above one or ten parameters are in good agreement with those of each crystal form. The discrepancies were within 2.5%.

The molecule has rotational freedom around the seven single bonds Co—C(9), C(9)—C(10), Co—P, P—C(12), P—C(18), P—C(24). If such rotations were introduced in the packing energy calculation the

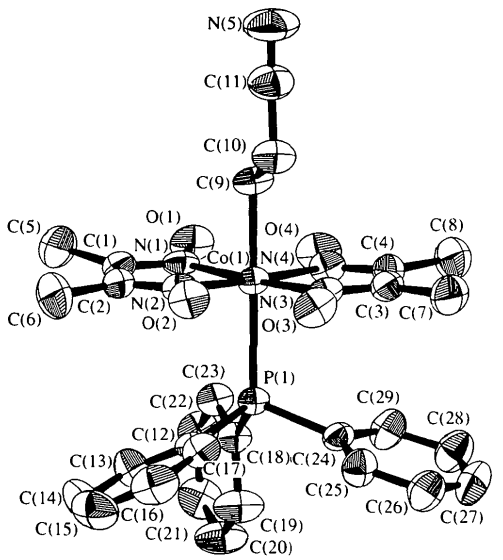

Fig. 8. Molecular structure of (I) with atom numbering. Displacement ellipsoids are drawn at the 50% probability level. H atoms are omitted for clarity.

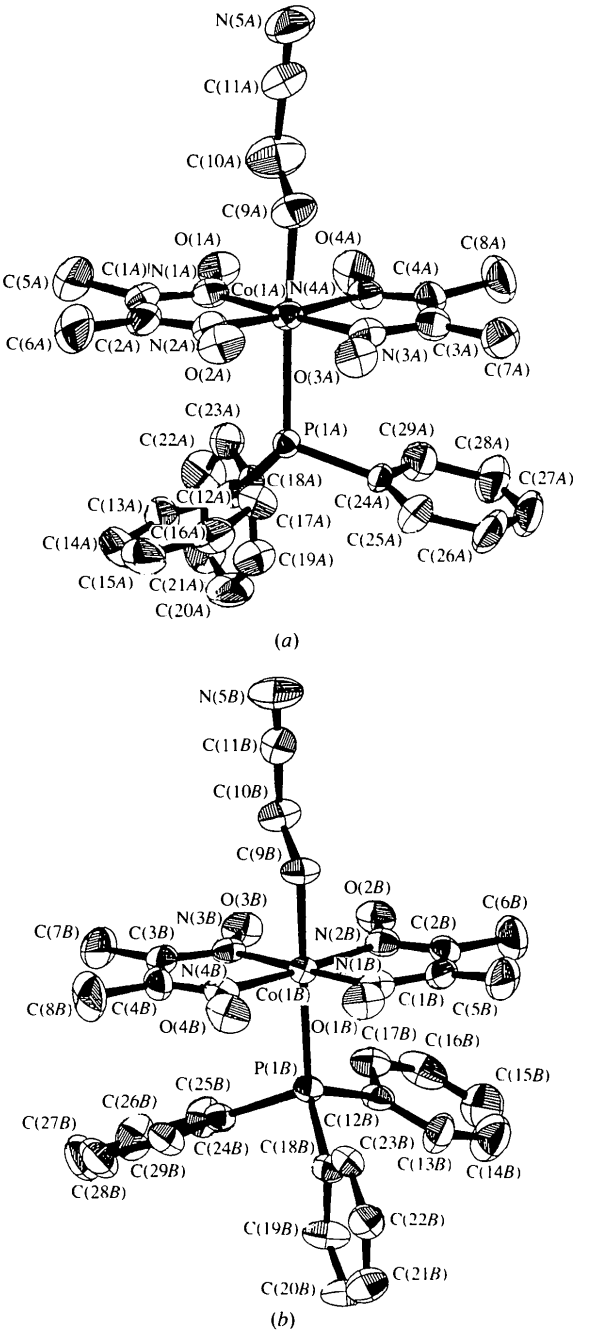

Fig. 9. Molecular structures: (*a*) *A* and (*b*) *B* of (II) with atom numbering. Displacement ellipsoids are drawn at the 50% probability level. H atoms are omitted for clarity.

converged structure and the energy may be different from the corresponding ones of the rigid model calculation. For form (IV), the packing energy calculation was performed by relaxing the conformations around the seven bonds. The converged structure is almost the same as the crystal structure and the energy became $-198.5\,kJ\,mol^{-1}$. These results suggest that the packing energies are approximately the same, within a few $kJ\,mol^{-1}$, among the different crystal forms.

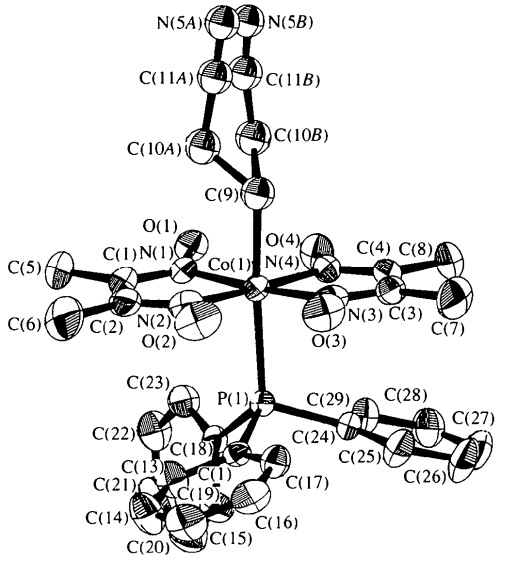

Fig. 10. Molecular structure of (III) with atom numbering. Displacement ellipsoids are drawn at the 50% probability level. H atoms are omitted for clarity. The ratio of *A* and *B* of the disordered moieties is 0.75 to 0.25.

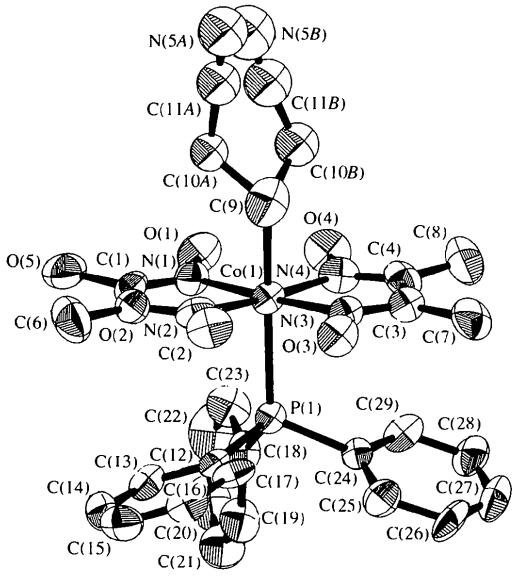

Fig. 11. Molecular structure of (IV) with atom numbering. Displacement ellipsoids are drawn at the 50% probability level. H atoms are omitted for clarity. The ratio of *A* and *B* of the disordered moieties is 0.59 to 0.41.

3.4. *Photoisomerization in the solid-state*

The 2-cyanoethyl group bonded to the Co atom is isomerized to the 1-cyanoethyl group when the powdered sample of the complex is irradiated with a xenon lamp. The changes of ν_{CN} of the 2-cyanoethyl group with exposure time for (I), (II) and (III) are shown in Fig. 15. The vertical axis is $\log(I_t/I_o)$, where I_t and I_o are the intensities of ν_{CN} after t s and before irradiation.

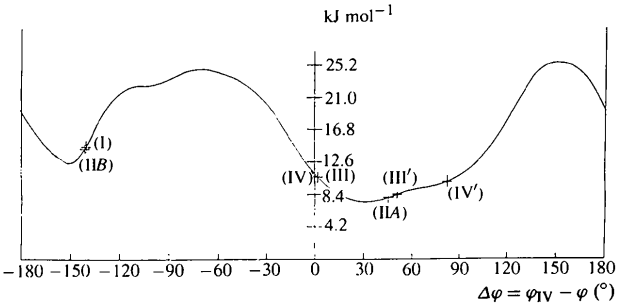

Fig. 12. Energy variation with rotation angle around the Co—O bond.

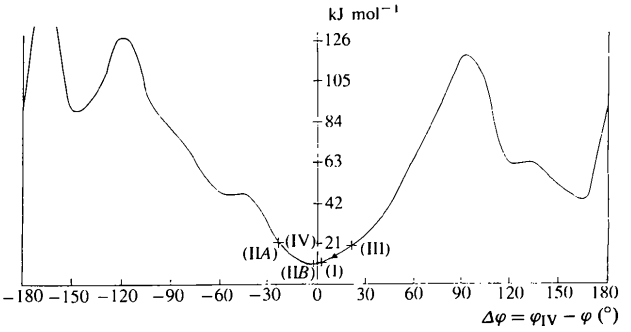

Fig. 13. Energy variation with rotation angle around the Co—P bond. The triangle indicates the angle observed in (*R*-1-cyanoethyl)-(triphenylphosphine)cobaloxime (Kurihara *et al.*, 1983).

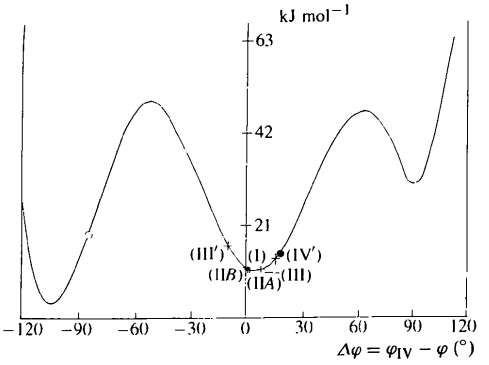

Fig. 14. Energy variation with rotation angle around the C(9)—C(10) bond. The open and full circles indicate the angle observed in the pyridine complexes with parallel and perpendicular conformations, respectively.

As shown in Fig. 15, the change is well explained by first-order kinetics. The rate constants were calculated to be 0.6×10^{-4}, 1.0×10^{-4} and 2.3×10^{-4} s^{-1} for (I), (II) and (III), respectively. The rate constants are significantly different among the three crystal forms.

3.5. *Reaction cavity*

In order to elucidate the relation between the reaction rate and the crystal structure, the reaction cavity for the 2-cyanoethyl group was calculated, which was defined in the crystalline-state racemization (Ohashi, Yanagi, Kurihara, Sasada & Ohgo, 1981). Fig. 16 shows the reaction cavity for each 2-cyanoethyl group. The volumes of the cavities were calculated to be 13.7, 10.9, 14.0, 15.7 and 19.0 Å^3, for the 2-cyanoethyl groups of (I), (II*A*), (II*B*), (III) and (IV), respectively. Form (II) has two crystallographically independent molecules, which have different reaction cavities. It seems quite plausible to assume that in the early stages the 2-cyanoethyl group with a larger reaction cavity may change more rapidly than that with a smaller cavity. The reaction rate of form (II), therefore, may depend on the larger reaction cavity.

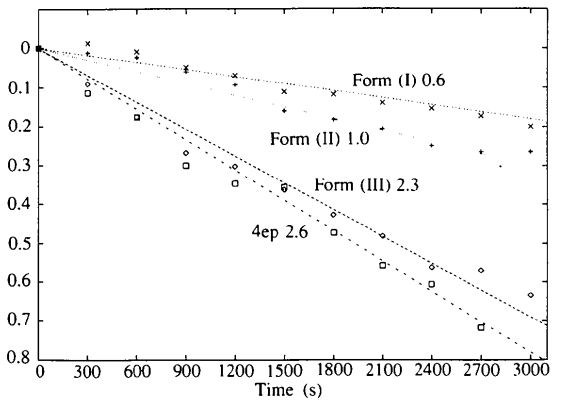

Fig. 15. Log plots of reaction rates for forms (I), (II) and (III). The reaction rate of the 4-ethylpyridine complex crystal (Sekine & Ohashi, 1991) was also measured in the same conditions to compare the rate constants with those of other cobaloxime complexes measured so far.

Although the rate constant of form (IV) has not been obtained, there is a quantitative relationship between the reaction rate and the reaction cavity. The rate constant of form (IV) is assumed to be $2–3 \times 10^{-4}$ s^{-1} from the relation. If we assumed that the compositions of the four crystal forms in the sample obtained by rapid crystallization are the same as those of crystals suitable for structure analysis, the composition ratio of (I):(II):(III):(IV) is 1:8:1:4. This indicates that approximately one third of the powdered sample (5/14) has a larger reaction cavity than that obtained by slow crystallization, in which the ratio of (I):(II) was 1:9. This is the reason why the powdered sample by rapid crystallization showed a significantly larger reaction rate than the sample by slow crystallization. It is noteworthy

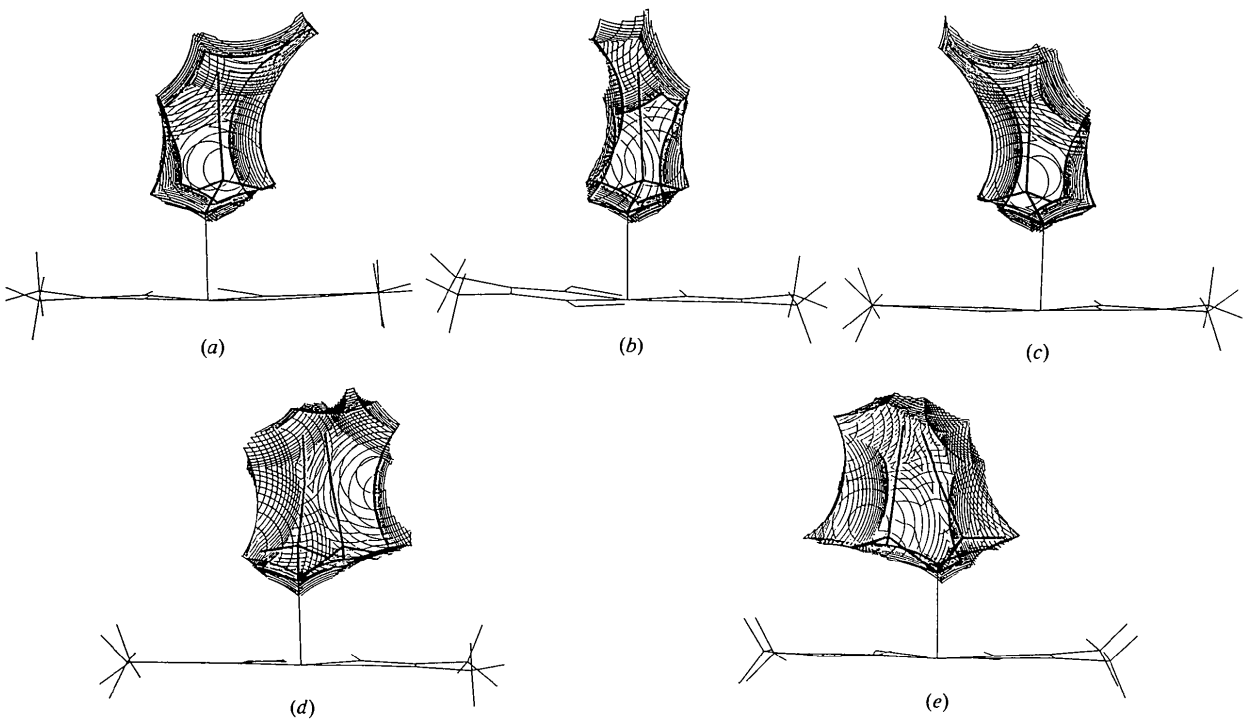

Fig. 16. Reaction cavities for the 2-cyanoethyl groups in four forms: (*a*) in (I), (*b*) *A* in (II), (*c*) *B* in (II), (*d*) in (III) and (*e*) in (IV). The volumes are 13.7, 10.9, 14.0, 15.7 and 19.0 Å^3, respectively.

that the 'pure' sample in the solid-state reaction should be composed of 'only one crystal form' and that it is distinct from the 'pure' sample in solution, in which different molecules are not included as impurities.

This work was partly supported by a Grant-in-Aid for Scientific Research from the Ministry of Education, Science and Culture, Japan. The authors are grateful to Professor Emeritus Yoshio Sasada and Dr Akira Uchida for kind suggestions.

References

Busing, W. R. (1981). *WMIN. A Computer Program to Model Molecules and Crystals in Term of Potential-Energy Functions*. Report ORNL-5747. Oak Ridge National Laboratory, Tennessee, USA.

Kurihara, T., Uchida, A., Ohashi, Y., Sasada, Y., Ohgo, Y. & Baba, S. (1983). *Acta Cryst.* B**39**, 431–437.

Ohashi, Y., Sekine, A., Shimizu, E., Hori, K. & Uchida, A. (1990). *Mol. Cryst. Liq. Cryst.* **186**, 37–44.

Ohashi, Y., Yanagi, K., Kurihara, T., Sasada, Y. & Ohgo, Y. (1981). *J. Am. Chem. Soc.* **103**, 5805–5812.

Ohgo, Y. & Takeuchi, S. (1985). *J. Chem. Soc. Chem. Commun.* pp. 21–23.

Schrauzer, G. N. & Windgassen, R. J. (1967). *J. Am. Chem. Soc.* **89**, 1999.

Sekine, A. & Ohashi, Y. (1991). *Bull. Chem. Soc. Jpn*, **64**, 2183–2187.

Sekine, A., Ohashi, Y. & Hori, K. (1991). *Acta Cryst.* C**47**, 525–528.

Sekine, A., Ohashi, Y., Shimizu, E. & Hori, K. (1991). *Acta Cryst.* C**47**, 53–56.

Sheldrick, G. M. (1985). *SHELXS86. Program for the Solution of Crystal Structures*. University of Göttingen, Germany.

Sheldrick, G. M. (1993). *SHELXL93. Program for the Refinement of Crystal Structures*. University of Göttingen, Germany.

Uchida, A., Danno, M., Sasada, Y. & Ohashi, Y. (1987). *Acta Cryst.* B**43**, 528–532.

Uchida, A., Ohashi, Y. & Ohgo, Y. (1991). *Acta Cryst.* C**47**, 1177–1180.

Williams, D. E. & Starr, T. L. (1977). *Comput. Chem.* **1**, 173–177.

Zangrando, E., Bresciani-Pahor, N., Randaccio, L., Charland, J.-P. & Marzilli, L. G. (1986). *Organometallics*, **5**, 1938–1944.